Postmortem radiological imaging of natural causes of death in adults – a review

Baumeister, Rilana ; Thali, Michael J ; Ampanozi, Garyfalia

Abstract: Radiological findings of natural causes of death in adults in postmortem imaging are of enormous value for medicolegal investigation. Postmortem computed tomography (PMCT) in particular is increasingly used as a triage tool after external inspection and before a full autopsy. Forensic pathologists and radiologists commonly deal with a wide variety of deaths from natural causes. The most common encountered natural causes of death refer to the cardiovascular, central nervous, respiratory, gastrointestinal and metabolic system. This review provides an overview of the literature on postmortem imaging of the major natural causes of death in adults, categorized by organ systems.

DOI: https://doi.org/10.1016/j.fri.2021.200473

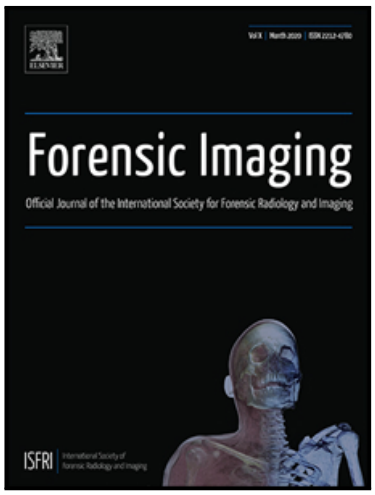

Postmortem radiological imaging of natural causes of death in adults – a review

Dr. Rilana Baumeister , J. Thali Michael , Garyfalia Ampanozi

PII: S2666-2256(21)00044-0
DOI: https://doi.org/10.1016/j.fri.2021.200473
Reference: FRI 200473

To appear in: *Forensic Imaging*

Received date: 8 January 2021
Revised date: 26 May 2021
Accepted date: 9 July 2021

Please cite this article as: Dr. Rilana Baumeister , J. Thali Michael , Garyfalia Ampanozi , Postmortem radiological imaging of natural causes of death in adults – a review, *Forensic Imaging* (2021), doi: https://doi.org/10.1016/j.fri.2021.200473

Highlights

- Natural causes of death represent a significant proportion of cases in forensic investigation
- Knowledge about imaging findings of natural causes of death is mandatory
- PMCT supports investigating fatalities in natural causes of death cases
- PMCT can be implemented as a triage tool

Postmortem radiological imaging of natural causes of death in adults – a review

Baumeister Rilana [a], Thali Michael J. [a], Ampanozi Garyfalia [a]

[a] University of Zurich, Institute of Forensic Medicine, Forensic Medicine and Imaging, Winterthurerstrasse 190/52, CH-8057 Zurich, Switzerland

Corresponding author:

Dr. Rilana Baumeister

University of Zurich

Institute of Forensic Medicine

Forensic Imaging and Virtopsy

Winterthurerstrasse 190/52

CH-8057 Zürich

Switzerland

e-mail: rilana.baumeister@irm.uzh.ch

tel.: +41 44 635 5611

Abstract

Postmortem radiological imaging of natural causes of death in adults – a review

Radiological findings of natural causes of death in adults in postmortem imaging are of enormous value for medicolegal investigation. Postmortem computed tomography (PMCT) in particular is increasingly used as a triage tool after external inspection and before a full autopsy.

Forensic pathologists and radiologists commonly deal with a wide variety of deaths from natural causes. The most common encountered natural causes of death refer to the cardiovascular, central nervous, respiratory, gastrointestinal and metabolic system.

This review provides an overview of the literature on postmortem imaging of the major natural causes of death in adults, categorized by organ systems.

Keywords

postmortem computed tomography, postmortem magnetic resonance imaging, Virtopsy, natural cause of death, forensic radiology

Abbreviations

PMCT, postmortem computed tomography; PMMR, postmortem magnetic resonance; PMCTA, PMCT angiography; PMMRA, PMMR angiography; SAH, subarachnoid hemorrhage; GRE, gradient recall echo; SWI, susceptibility-weighted imaging; HU, Hounsfield Units;

Introduction

Postmortem imaging has been a growing topic over the last three decades, and the use of forensic radiology has increased worldwide in the field of forensic medicine [1-3].

Postmortem computed tomography (PMCT) and, to a lesser extent, PMCT angiography (PMCTA), postmortem magnetic resonance (PMMR), PMMR angiography (PMMRA) and image-guided biopsies are established imaging methods in several medicolegal centers worldwide [1, 3-6].

Several forensic institutions routinely use PMCT [3], because of its excellence in identifying foreign bodies including projectiles, depicting skeletal fractures, detecting gas and hemorrhage [7, 8], and it also has its contribution to natural causes of death [6, 9]. Due to PMCT's reduced ability to depict vascular lesions and to differentiate soft tissue interfaces, PMCTA, PMMR and PMMRA were introduced in subsequent years as an adjunct to autopsy [3, 5, 6, 10, 11]. In particular, PMCTA as a complementary tool to whole-body PMCT shows its value when natural causes of death are suspected and where unenhanced PMCT might not accurately document or identify pathologic alterations [12]. Even though not every institution has the possibility, feasibility and equipment for PMCTA and PMMR, there are low-cost options for PMCTA by enteroclysis pumps or PMCTA kits [13, 14].

In our institution, PMCT as a triage tool after external inspection and before full autopsy has been established since 2015. In cases of a natural cause of death, this tool helps to avoid additional, cost-intensive examination and autopsy [15].

Forensic pathologists deal with homicidal or accidental deaths but in most cases, investigate a wide range of deaths from natural causes [16]. In 2015, more than 40% of all cases who were investigated in our institute were of natural causes, which is the majority of cases and therefore worth focusing on in this review. The variety of natural causes of death is large, e.g., cardiac arrest due to infarction, central nervous infarction due to bleeding or respiratory failure due to infection, to name only a few [6].

This review provides an overview of the literature referring to postmortem radiological imaging of the most important natural causes of death in adults divided by organ systems.

Cardiovascular system

Cardiomegaly

Cardiomegaly is considered a frequent cause of sudden death [17]. There have been efforts to perform in situ heart measurements, since their usefulness as indicators for heart disease is very well known [18]. Heart weight, as a marker of cardiomegaly, can be estimated both on PMCT [19] and PMMR [20] by assessing the circumferential area of the left heart ventricle, allowing for prediction of the actual heart weight. Further studies have either set new thresholds for the cardiothoracic ratio on PMCT [21] or proposed new formulas based, among others, on the cardiothoracic ratio on PMCT [22], both intending to predict cardiomegaly. Winklhofer et al. concluded that a specificity of 95% in diagnosing cardiomegaly can be achieved if the PMCT cardiothoracic ratio threshold of 0.57 is set [21]. It is, however, important not to compare postmortem imaging heart measurements to normal value tables established by autopsy measurements. Normal values referring to postmortem imaging cardiac measurements still have to be defined. It was found that cardiac PMMR assessment of myocardial wall thickness tends to overestimate the actual autopsy measurements [23, 24].

Ischemic heart disease

Although myocardial infarction is the most frequently encountered cause of death from the cardiovascular system, it is barely depicted by unenhanced PMCT. Indirect signs of possibly existing indicators for sudden cardiac death, such as coronary artery calcification, past bypass operation, stents in the coronary arteries, or calcified scars of previous myocardial infarctions, are only suggestive and not substantial evidence of myocardial infarction. Rare findings correlated with cardiac ischemia, such as myocardial bridges [25] or coronary artery anatomic anomalies [26], can be revealed by postmortem imaging.

In contrast, there is strong evidence in the literature that PMMR is the best modality for the preautopsy depiction of this pathological entity [27, 28]. PMMR not only enables identification of the infarction area but also provides evidence for its age. The distinction between acute, subacute and chronic infarction can be based on T2-weighted images with central hypointese areas with peripheral hyperintense margins, hyperintese, and hypointense areas, respectively [28]. Even peracute myocardial infarctions are diagnosable on PMMR as hypointense regions, a finding of great importance, as these myocardial lesions are not yet macroscopically identifiable [28]. Knowing their presence and exact localization before autopsy can lead to targeted histological probing during autopsy or with guided biopsy. Actually, the combination of PMMR and guided biopsy of the myocardium provides the highest accuracy in the preautopsy diagnosis of acute or chronic myocardial ischemia [29].

Ischemic heart disease can also be depicted by PMCTA (either whole body or targeted) in terms of pathological myocardial enhancement [30, 31]. Severe coronary artery stenosis and occlusions are easily identifiable with PMCTA [12, 32-34] and therefore a valuable tool in cases of sudden cardiac death, even if the exact pathomorphological explanation cannot always be provided [34]. Cardiac PMMR examinations also provide tools for the assessment of coronary artery

patency. Ruder et al. described the presence of chemical shift artefact as an indicator for patency and paired dark bands as a finding related to coronary stenosis [35].

Hemopericardium

The presence of blood in the pericardial sac (hemopericardium) is identifiable on unenhanced PMCT. However, the diagnosis of pericardial tamponade is primarily clinical. Postmortem signs indicating a fatal hemopericardium and thus a pericardial tamponade have been described: target sign, flattening of the right ventricular wall and coronary sinus and pulmonary artery compression, and, to a lesser extent, hepatic and renal vein distension [36]. Referring to the target sign, or armored heart sign, Shiotani et al. described it as the most frequently observed PMCT finding in cases of aortic dissection leading to hemopericardium [37], and Watanabe et al. proposed it as a sign of a fatal pericardial tamponade, since its origin can be explained by a beating myocardium [38].

Although PMCTA and PMMR are the methods of choice in identifying the cause of the hemopericardium [12, 39, 40], unenhanced PMCT can very often be suggestive of it, particularly for the differentiation between ruptured myocardial infarction and ruptured aortic dissection [41] (Figure 1).

Pulmonary thromboembolism

Pulmonary thromboembolism is frequently encountered in forensic institutes since it is considered a sudden, unexpected death because of the acute onset of symptoms. Postmortem formation of clots hinders a definite diagnosis of pulmonary thromboembolism on unenhanced PMCT. Centrally located hyperdense material in the pulmonary trunk and in the main pulmonary arteries raises the suspicion and can be mistaken by inexperienced readers. In a minimally invasive manner, PMCTA will reveal contrast medium filling defects

in both cases (postmortem clots and thromboembolism), and PMCT-guided biopsy will finally lead to the diagnosis [42, 43]. Recently, indirect findings have been proposed as indicators of pulmonary thromboembolism. Perivascular edema of the lower extremities and a distinct irregular shape of the pulmonary trunk and artery content [44] in combination with venous vessel congestion [45] are rated as strongly suggestive of pulmonary thromboembolism on unenhanced PMCT. PMMR has also been described as an adjunct in the preautopsy diagnosis of pulmonary thromboembolism [46, 47], with promising results. However, larger studies are still needed for this pathological condition.

Aortic dissection, Aortic aneurysm

Both pathological entities are well depicted on postmortem imaging. The type and localization of an aortic dissection will define the outcome. Classification according to the Stanford system is the most widely used, with type A describing dissections of the ascending aorta and type B describing dissections distal to the left subclavian artery [48]. Dislocated calcification towards the aortic lumen, intimomedial flap depiction (without calcification) and the double sedimentation sign (uneven sedimentation level between true and false aortic lumen) are identifiable on unenhanced PMCT [49] and allow for the diagnosis of aortic dissection. Involvement of the coronary arteries (in type A dissections) or rupture of the adventitia and blood exsanguination into the pericardial sac, the pleural or the abdominal cavity are the most frequently encountered causes of death. PMCTA allows for a definitive diagnosis and documentation of this pathological finding [12], and PMMR also clearly demonstrates the dissection membrane [50].

Aortic aneurysms are identified as enlargements of the diameter of the aorta, and they can lead to massive blood loss in cases of rupture. PMCT is the method of choice for identifying this pathology as the cause of death [51-53], with PMCTA

also enabling the exact localization of the rupture site [15]. This is of great significance in cases of triage [15] or for optimized planning of the autopsy.

Gastrointestinal system

Natural causes of death from the gastrointestinal system refer mostly to intestinal obstruction and gastrointestinal bleeding; however, they are rather rarely encountered in a forensic setting.

Bowel obstruction

In 80% of all cases, the etiology of bowel obstruction refers to adhesions, hernias and malignancies [54]. A case history of abdominal pain, vomiting (bilious to feculent), abdominal distension, and fever is highly suspicious for this pathological entity [55]. If left without medical care, bowel obstruction will lead to intestinal strangulation, ischemia with or without perforation, necrosis and finally sepsis [54, 55]. The referred sensitivity and specificity of computed tomography in living patients reaches 95% for detecting bowel obstruction, with the main findings being dilatation of the proximal part and decompression of the distal part of the bowel [54].

A special form of bowel obstruction is closed-loop obstruction [54] or volvulus, which can practically be found along the gastrointestinal tract; however, it is commonly encountered in the sigmoid colon. Specific radiological signs, such as the “bird beak” (the transition between distended to narrowed lumen [56]), the “coffee bean” (distended closed loop [56]) or the “whirlpool” (twisting of the mesenterium with vessels) sign [57], allow for a diagnosis. It is very interesting that these signs have also been described in unenhanced PMCT [58-60].

Gastrointestinal hemorrhage

Ulcers, esophageal varices, and neoplasms account for the vast majority of upper gastrointestinal hemorrhages, whereas hemorrhoids, colitis, diverticular

disease, neoplasms and angiodysplastic lesions account for lower gastrointestinal bleeding [61]. PMCT is a valuable tool for the diagnosis of gastrointestinal bleeding. Hyperdense stomach and/or intestine content, usually with clot formation, is the main finding [62-64] (Figure 2). Differentiation of blood clots from other hyperdense stomach contents might be challenging in some cases. Sudden onset of the hemorrhage or onset over longer time intervals seem to have an impact on the postmortem radiological appearance of gastrointestinal hemorrhage [65]. PMCTA is the method of choice if exact localization of the bleeding source should be identified [63, 66, 67].

Central nervous system

Intracranial hemorrhage

Intracranial hemorrhage remains a cause of significant morbidity and mortality [68]. It is an encompassing term characterized by the extravascular accumulation of blood within different intracranial spaces. Intracranial hemorrhage presents as hyperattenuation in parenchymal, subarachnoid, subdural, intraventricular, or epidural locations [69]. The most common causes of intracranial hemorrhage are trauma, hemorrhagic stroke, hypertension and ruptured aneurysm [70]. Complications include hematoma expansion and intraventricular components, increased intracerebral pressure as a result of the hemorrhage itself, stroke, and hydrocephalus, which is due to obstruction of cerebrospinal fluid or surrounding edema [68].

In postmortem imaging of the brain, classic anatomy disappears: there is loss of differentiation of gray and white matter, sulci and gyri and unidentifiable ventricles. However, discriminating intraparenchymal hemorrhages from extraaxial hemorrhages appears to be relevant with regard to the manner of death with a focus on further investigation of the case [71].

In this review, we present the two most common intracranial hemorrhages, which we encounter routinely and cause natural death.

Subarachnoid hemorrhage

Characteristic findings of extraaxial subarachnoid hemorrhage (SAH) are increased attenuation along the tentorium cerebelli and in the basal cisterns, sylvian fissure, and subarachnoid space on brain CT scans, often combined with intraventricular components [72] that are due to trauma or ruptured aneurysms. In postmortem imaging, these characteristics are detected frequently, but later after conventional autopsy, they cannot be confirmed and thus corrected to pseudo-SAH. This sign is often seen in association with brain swelling, hypoxic ischemic encephalopathy, global ischemia and venous congestion. In contrast, true SAH is more common in cases with asymmetric acute/subacute intraventricular and intraparenchymal hemorrhage and a history of anticoagulation therapy. Thus, pseudo-SAH is a diagnostic pitfall not only on antemortem but also on postmortem CT [73]. Figure 3 and 4 show PMCT images of true and pseudo-SAH.

Intraparenchymal hemorrhage

Intracerebral hemorrhage occurs twice as often as SAH and is equally as fatal. Common risk factors include hypertension, cerebral amyloid angiopathy, advanced age, antithrombotic therapy, drug abuse and history of cerebrovascular disease. Hematoma locations are deep or ganglionic, lobar, cerebellar, and brain stem in descending order of frequency [74].

Charcot-Bouchard aneurysms, believed to result from lipohyalinosis of small arterioles, are often blamed for the rupture of small penetrating blood vessels implicated in intracerebral hemorrhage involving the cerebellum, pons, thalamus and basal ganglia [68].

In postmortem radiology, forensic enlightenment is demanding, and according to Nolte et al., cocaine abuse is responsible for intracerebral hemorrhage in approximately 70% of cases with a mean age of 39 years [75]; thus,

toxicological examination in younger deceased with parenchymal hemorrhage should be considered.

On magnetic resonance imaging, the most important sequences in the evaluation of hemorrhage are gradient recall echo (GRE) and susceptibility-weighted imaging (SWI), whereas SWI is more sensitive than GRE in the detection of parenchymal hemorrhage [69].

In the first days after death, there is no relevant difference in radiological appearance in most findings in ante- or postmortem brains [76]. However, Berger et al. demonstrated in 2015 that subdural hematomas became denser and shrank postmortem; thus, their appearance changes. This might indicate that hematomas may appear more acute than they actually are and makes age determination of hemorrhage even more challenging [77]. Therefore, it is advantageous to be familiar with pitfalls in the imaging interpretation of intracranial hemorrhages for both the living and deceased. Although postmortem imaging might have a different radiological appearance than clinical imaging, the overall specificity for intra- and extraaxial brain findings without putrefaction compared to autopsy was 94% for PMCT and PMMR [76]. Tappero et al. even showed the possibility of detecting and localizing intracranial hemorrhage in putrefied bodies of at least 5 mm extent. The reason was the higher density of blood relative to brain tissue (74.67 Hounsfield Units (HU) +/- 5.43 SD, 42.01 HU +/- 3.75 SD, respectively). However, the cause of intracranial hemorrhage might remain unclear with putrefaction and hemorrhage shifting and relocating over time [71].

In general, values greater than 100 HU should correspond to anything else than hemorrhage, but overlapping may occur; thus, differentiation might also be challenging [69, 73, 77]. In those cases, an additional PMMR might help differentiation. Hemorrhage mimickers, for instance, are calcifications that can be discriminated by SWI sequence, the philtered-phase sequence [69].

Above mentioned PMMR is a powerful diagnostic tool in diagnosing intracranial hemorrhage; it is more sensitive than PMCT in the detection of subarachnoid hemorrhagic localizations, whereas no significant difference resulted from the detection of epidural and subdural hemorrhagic findings [5, 78]. Furthermore, detection of intraventricular hemorrhage by PMCT or PMMR is superior to autopsy [76]. Extraaxial hemorrhages were visible on both PMMR and PMCT in approximately 90% of all cases. Nevertheless, it is important to note that thin layers of blood may be invisible on cross-sectional imaging, and findings smaller than 3 mm regularly escaped the radiologist's analysis [5, 76, 78, 79].

Infections

Infections of the nervous system (CNS) are potentially life-threatening with high morbidity and mortality and are caused by pathogens such as bacteria, viruses, and fungi. CNS infections primarily involve meninges and parenchymal structures in the form of meningitis, encephalitis, and brain abscesses [80]. Predisposing factors for infections include usually diabetes mellitus and immune deficiency [81].

Native CT and MR imaging findings in meningitis are nonspecific and encompass subdural effusions, ventricular debris, hydrocephalus and high signal changes on diffusion-weighted MR imaging (DWI) and infarcts, for example, with MR being superior to CT in the detection of meningeal pathology [82]. Clinical causes of cerebral infections, including meningitis and especially tuberculous meningitis with hydrocephalus and bilateral basal ganglia infarctions [82, 83], might be visible in postmortem imaging. Cerebral infarcts newly discovered in postmortem imaging might also indicate infectious systemic diseases such as pneumonia, endocarditis or sepsis [84]. However, in routine PMCT it is difficult to make a clear diagnosis of cerebral infection.

Further, often focal infection is a brain abscess, it is a rare but potentially lethal infection of the brain parenchyma, and Staphylococcus aureus is the most commonly responsible pathogen [81]. In PMCT, abscess usually shows a well-defined, centrally hypodense lesion with a hyperdense ring, surrounding edema [85], antemortem even with well-known ring enhancement after contrast admission. Brain abscesses often originate from sinusitis, otitis, dental infection, cranial trauma with osseous defects and direct migration to the brain parenchyma. It is also a known complication of surgically treated intracerebral hemorrhage but is rare in cases of non-operated intracerebral hemorrhage. Hematogenous spread arises from distant foci (especially pneumonia and infectious endocarditis) [81]. Thus, Chatzaraki et al. state that early detection of potentially infectious foci enables forensic pathologists to take appropriate protective measures and to adapt their approach during autopsy [85].
Differential diagnoses of brain abscess are brain tumors and metastasis, which PMMR and PMCTA might help to differentiate [85]. Another tool for differentiation is currently postmortem MR spectroscopy as an evolving tool. Some possibilities of its use have already been reported in postmortem setups [86, 87], and further investigations are needed. In clinical use, MR spectroscopy is already established and shows lactate peaks in the center of an abscess [81] and also Amino acids at 0.9 ppm [88].
Thurnher and Sundgren recommend differentiating tuberculomas from pyogenic brain abscesses by use of MR spectroscopy in the living [82], in addition, another distinction can be made between anaerobic and aerobic bacteria, as well as parasite and fungicide origin [88, 89].

Respiratory system

Imaging reporting of the lungs in the postmortem setting is challenging because of the normal postmortem findings, e.g., dependent density, unspecific ground glass attenuation and consolidation [90]. The postmortem detection of

pulmonary pathologies is sometimes limited to the extent of ventilation; thus, some studies have investigated the ability to increase the sensitivity of PMCT for pulmonary findings by performing data acquisition during pulmonary ventilation in some deceased [91, 92]. Ventilation is a proper tool to distinguish mal ventilated and consolidated lung areas from normal postmortem findings and additional pathologies such as pneumonia or tumors [91, 93]. Equipment and pitfalls, including movement artifacts and gastric dilatation, are limitations of this method [91].

Pneumothorax

Detection of a pneumothorax is obvious in PMCT and is often seen at our institute, especially in putrefied bodies. Pneumothorax is defined as the presence of free air within the pleural space. It can be spontaneous, traumatic and putrefaction-related or iatrogenic. For example, spontaneous pneumothorax has been associated with emphysema-like changes and the presence of bullae, more often located in the upper lungs. There is evidence that spontaneous pneumothorax is associated with smoking and chronic obstructive pulmonary disease. Detection of this pathological entity is quite simple in PMCT but not easy at autopsy since it requires a special examination procedure and can therefore easily be missed [94, 95]. Though mortality rates of pneumothorax alone are relatively low [96], in our experience, it is often seen in PMCT whether in traumatic cases, decomposed bodies or postinterventional.

Pneumonia

Pneumonia is one of the most common pathologies in the lung and remains a leading cause of hospitalization and the fourth leading cause of death worldwide [97] or contributes to severe complications such as sepsis with multiorgan failure and death. Risk factors are increased age, comorbidities, immune deficiency, alcohol abuse, corticosteroid use, and even genetic factors [98].

A common main differentiation of pneumonias includes community-acquired and hospital-acquired pneumonia. Bacterial infection with Streptococcus pneumoniae is the most common pathogen, with 25%, causing community-acquired pneumonia.

Another important pathogen causing pneumonia is Mycobacterium tuberculosis (TB), which latently affects approximately a quarter of the world's population according to World Health Organization [97]. TB is one of the ten leading causes of death worldwide [99] and can affect almost any part of the body but is mainly an infection of the lungs, producing cavitating lung lesions in the apices and upper lobes, well-defined centrilobular nodules, and tree-in-bud signs visible on PMCT. An important complication of TB-associated pneumonia is lethal hemoptysis [16, 100].

Additionally, there are still many other pathogens, such as fungi and viruses, which cause pneumonia. Recently, COVID-19 virus pandemic has influenced the world and, even though many supportive therapeutics are available [101].

The radiographic appearance of pneumonia varies greatly and might be challenging postmortem because of density-related changes or additional pleural effusion that compresses the pulmonary lower lobe. Lobar consolidation, ground glass opacities, interstitial infiltrates or pulmonary abscesses might be detectable [98]. Figure 5 shows a case of aspiration pneumonia in the left lower lobe.

Traill reported in 2010 that common major errors on thoracic imaging are missed diagnoses of pneumonia, a common cause of natural causes of death [102]. Recently, Gonoi et al. published helpful characteristics to identify pneumonia on unenhanced PMCT, e.g., associations with segmental and centrilobular opacities in pneumonia [103].

PMCT can alert pathologists to possible dangerous communicable infections such as tuberculosis and allow them to take adequate protective measures during autopsy such as personal protective equipment in a special high-risk autopsy suite with appropriate ventilation [104].

Cancer

Malignancies are one of the most commonly encountered causes of death in addition to cardiovascular causes and stroke, and they are still increasing despite new improved diagnostics and therapies [97, 105, 106].

In this review, we can only give a brief overview of this vast topic.

The most prevalent cancer is lung cancer, with a low survival time and high mortality depending on the subtype. The most important risk factor is smoking tobacco in addition to genetic alterations [107, 108].

Although sometimes the diagnosis of cancer remains undetected, postmortem imaging might reveal malignancy and can correlate with autopsy.

Metastases are frequently seen, most often in the liver, lungs, bones and brain [107], and stay visible postmortem. Bone metastasis originates most commonly from breast and prostate cancer as well as lung and thyroid cancer and might be osteolytic or osteoblastic. Figure 6 shows bone metastasis originating from prostate cancer in an older male deceased after therapy; note the mixed radiological appearance of osseous metastasis, which is due previous therapy.

Any malignant tumor may metastasize to the bone. Bone metastasis from occult carcinoma more often causes harm and further pathologies, e.g., pathologic fractures and spinal metastasis with cord compression [107].

Cancer is one of the most important causes of death in recent times [97, 105, 106, 109], and it can still stay undetected [110]. A recent work by Vester et al. identified that the most common cause of death in an out-of-hospital population was cancer (62%), and the causes of death for a few cases were not known by their general practitioners [111].

Occult carcinomas, frequently originating from the lung, liver, pancreas and gastrointestinal tract, often show bone metastasis as the first pathology and sometimes can only be detected by extensive clinical investigation or final autopsy but often remain unknown [107].

O'Brien et al. reported a case of pulmonary tumor thrombotic microangiopathy, which mostly was due to gastric adenocarcinomas but also to breast, pancreas and lung cancers that caused rapidly progressive pulmonary hypertension and fatal ends. Postmortem imaging revealed previously unknown signet ring cell gastric adenocarcinoma with metastasis in lymph nodes and other organs [112]. Takahashi et al. described a case dying from asphyxia caused by unknown metastatic lung and endobronchial tumors revealed by PMCT [113] and pointed out the usefulness of postmortem imaging.

Metabolic dysfunction

Diabetes mellitus

Diabetes mellitus is a chronic, metabolic disease defined by increased blood glucose with more than 420 million people affected worldwide. It is a major cause of nerve damage, blindness, kidney failure, heart attacks, stroke and lower limb amputation because of microvascular damage and increases the risk of further macrovascular complications [114]. If the forensic pathologist is unaware of the medical history at the time of the autopsy, the diagnosis might be missed [115]. In such a case, prior PMCT is a very helpful tool to uncover several diabetes-associated imaging findings, even though they are not specific for the disease [116]. Bilateral mural calcification of the vas deferens (Figure 7) is the radiological tell-tale sign for diabetes, with a prevalence of approximately 10% in diabetic males [117-119].

Further PMCT findings associated with diabetes include obese stature, adrenal adenomas, decreased liver density, calcified plaques in coronary, renal and lower extremity arteries, renal atrophy, left ventricular hypertrophy and urinary bladder overdistension [116].

In cases where imaging findings from preautopsy PMCT are suggestive for diabetes, forensic pathologists can actively search for organ changes related to diabetes during autopsy, order biochemical tests to confirm the diagnosis based

on glycosylated hemoglobin (HbA1c), assess glucose and lactate levels in the cerebrospinal fluid, glucose and acetone in the urine, and glycated hemoglobin levels in the blood to diagnose fatal diabetic hypoglycemia or hyperglycemia [115]. Diabetic ketoacidosis as a metabolic complication might end lethally if untreated.

Heimer et al. recently described the method of postmortem hydrogen proton MR spectroscopy, which is able, noninvasively, to measure pathological metabolite concentrations in small volumes in the brain in addition to conventional autopsy [86].

However, conclusive distinction in daily routine requires biochemical and toxicological analysis of blood and urine samples.

Conclusion

Natural causes of death are the most common causes of death in the field of forensic medicine and forensic radiology and constitute a large part of the knowledge in this field. Every forensic radiologist or forensic pathologist who reports radiological findings in postmortem imaging should be familiar with normal anatomy and appearance in both the deceased and living to note pathologies that cause natural death. By visualization of postmortem imaging, we are able to detect common natural causes of death even without autopsy. This enhances PMCT as a triage tool.

Acknowledgments

The authors express their gratitude to Emma Louise Kessler, MD, for her generous donation to the Zurich Institute of Forensic Medicine, University of Zurich, Switzerland.

Funding

This work did not receive any specific grant from funding agencies in the public, commercial, or not-for-profit sectors.

References

1. O'Donnell C, Woodford N. Post-mortem radiology--a new sub-speciality? Clin Radiol. 2008;63(11):1189-94.
2. Okuda T, Shiotani S, Sakamoto N, Kobayashi T. Background and current status of postmortem imaging in Japan: short history of "Autopsy imaging (Ai)". Forensic Sci Int. 2013;225(1-3):3-8.
3. Grabherr S, Grimm J, Dominguez A, Vanhaebost J, Mangin P. Advances in post-mortem CT-angiography. The British Journal of Radiology. 2014;87(1036):20130488.
4. Flach PM, Gascho D, Schweitzer W, Ruder TD, Berger N, Ross SG, et al. Imaging in forensic radiology: an illustrated guide for postmortem computed tomography technique and protocols. Forensic Sci Med Pathol. 2014;10(4):583-606.
5. Ruder TD, Thali MJ, Hatch GM. Essentials of forensic post-mortem MR imaging in adults. Br J Radiol. 2014;87(1036):20130567.
6. Grabherr S, Egger C, Vilarino R, Campana L, Jotterand M, Dedouit F. Modern post-mortem imaging: an update on recent developments. Forensic Sci Res. 2017;2(2):52-64.
7. Filograna L, Pugliese L, Muto M, Tatulli D, Guglielmi G, Thali MJ, et al. A Practical Guide to Virtual Autopsy: Why, When and How. Semin Ultrasound CT MR. 2019;40(1):56-66.
8. Smith APT, Traill ZC, Roberts ISD. Post-mortem imaging in adults. Diagnostic Histopathology. 2018;24(9):365-71.
9. Blokker BM, Wagensveld IM, Weustink AC, Oosterhuis JW, Hunink MG. Non-invasive or minimally invasive autopsy compared to conventional autopsy of suspected natural deaths in adults: a systematic review. European Radiology. 2016;26(4):1159-79.
10. Thali MJ, Yen K, Schweitzer W, Vock P, Boesch C, Ozdoba C, et al. Virtopsy, a new imaging horizon in forensic pathology: virtual autopsy by postmortem multislice computed tomography (MSCT) and magnetic resonance imaging (MRI)--a feasibility study. J Forensic Sci. 2003;48(2):386-403.

11. Jackowski C, Sonnenschein M, Thali MJ, Aghayev E, von Allmen G, Yen K, et al. Virtopsy: postmortem minimally invasive angiography using cross section techniques--implementation and preliminary results. J Forensic Sci. 2005;50(5):1175-86.
12. Ross SG, Bolliger SA, Ampanozi G, Oesterhelweg L, Thali MJ, Flach PM. Postmortem CT angiography: capabilities and limitations in traumatic and natural causes of death. Radiographics. 2014;34(3):830-46.
13. Vester MEM, Servaas E, Beenen LFM, Clerkx M, de la Rie A, Lobé NHJ, et al. Feasibility of an enteroclysis pump for post-mortem computed tomography angiography (PMCTA). Forensic Imaging. 2020;20:100340.
14. Schweitzer W, Enders M, Thali M. Very affordable post mortem CT angiography kit: Feasibility study using immersion pump and 3D printed parts. Journal of Forensic Radiology and Imaging. 2019;16:11-8.
15. Chatzaraki V, Heimer J, Thali M, Dally A, Schweitzer W. Role of PMCT as a triage tool between external inspection and full autopsy – Case series and review. Journal of Forensic Radiology and Imaging. 2018;15:26-38.
16. Hugar BS, Jayanth SH, Girish Chandra YP, Udaya Shankar BS. Sudden death due to massive hemoptysis secondary to pulmonary tuberculosis – A case report. Journal of Forensic and Legal Medicine. 2013;20(6):632-4.
17. Tavora F, Zhang Y, Zhang M, Li L, Ripple M, Fowler D, et al. Cardiomegaly is a common arrhythmogenic substrate in adult sudden cardiac deaths, and is associated with obesity. Pathology. 2012;44(3):187-91.
18. Michaud K, Genet P, Sabatasso S, Grabherr S. Postmortem imaging as a complementary tool for the investigation of cardiac death. Forensic Sci Res. 2019;4(3):211-22.
19. Hatch GM, Ampanozi G, Thali MJ, Ruder TD. Validation of left ventricular circumferential area as a surrogate for heart weight on postmortem computed tomography. Journal of Forensic Radiology and Imaging. 2013;1(3):98-101.
20. Ruder TD, Stolzmann P, Thali YA, Hatch GM, Somaini S, Bucher M, et al. Estimation of heart weight by post-mortem cardiac magnetic resonance imaging. Journal of Forensic Radiology and Imaging. 2013;1(1):15-8.
21. Winklhofer S, Berger N, Ruder T, Elliott M, Stolzmann P, Thali M, et al. Cardiothoracic ratio in postmortem computed tomography: reliability and threshold for the diagnosis of cardiomegaly. Forensic Sci Med Pathol. 2014;10(1):44-9.
22. Jotterand M, Faouzi M, Dédouit F, Michaud K. New formula for cardiothoracic ratio for the diagnosis of cardiomegaly on post-mortem CT. Int J Legal Med. 2020;134(2):663-7.
23. Ampanozi G, Hatch GM, Flach PM, Thali MJ, Ruder TD. Postmortem magnetic resonance imaging: Reproducing typical autopsy heart measurements. Leg Med (Tokyo). 2015;17(6):493-8.

24. Chatzaraki V, Thali MJ, Schweitzer W, Ampanozi G. Left myocardial wall measurements on postmortem imaging compared to autopsy. Cardiovasc Pathol. 2019;43:107149.
25. Ampanozi G, Gascho D, Hatch G, Schulze C, Thali MJ, Ruder TD. What is unsought will go undetected – Myocardial bridging on postmortem computed tomography. Journal of Forensic Radiology and Imaging. 2014;2(1):5-8.
26. Martinez RM, Flach PM, Ebert LC, Bartsch C, Thali MJ, Ampanozi G. Anomalous left coronary artery origin on postmortem imaging in correlation with autopsy. Journal of Forensic Radiology and Imaging. 2014;2(3):146-8.
27. Jackowski C, Christe A, Sonnenschein M, Aghayev E, Thali MJ. Postmortem unenhanced magnetic resonance imaging of myocardial infarction in correlation to histological infarction age characterization. European heart journal. 2006;27(20):2459-67.
28. Jackowski C, Schwendener N, Grabherr S, Persson A. Post-mortem cardiac 3-T magnetic resonance imaging: visualization of sudden cardiac death? Journal of the American College of Cardiology. 2013;62(7):617-29.
29. Wagensveld IM, Blokker BM, Pezzato A, Wielopolski PA, Renken NS, von der Thüsen JH, et al. Diagnostic accuracy of postmortem computed tomography, magnetic resonance imaging, and computed tomography-guided biopsies for the detection of ischaemic heart disease in a hospital setting. European heart journal cardiovascular Imaging. 2018;19(7):739-48.
30. Vanhaebost J, Ducrot K, de Froidmont S, Scarpelli MP, Egger C, Baumann P, et al. Diagnosis of myocardial ischemia combining multiphase postmortem CT-angiography, histology, and postmortem biochemistry. La radiologia medica. 2017;122(2):95-105.
31. Sabatasso S, Vanhaebost J, Doenz F, Palmiere C, Michaud K, Dedouit F, et al. Visualization of Myocardial Infarction in Postmortem Multiphase Computed Tomography Angiography: A Feasibility Study. The American Journal of Forensic Medicine and Pathology. 2018;39(2).
32. Saunders SL, Morgan B, Raj V, Robinson CE, Rutty GN. Targeted post-mortem computed tomography cardiac angiography: proof of concept. International Journal of Legal Medicine. 2011;125(4):609-16.
33. Roberts ISD, Benamore RE, Peebles C, Roobottom C, Traill ZC. Diagnosis of coronary artery disease using minimally invasive autopsy: evaluation of a novel method of post-mortem coronary CT angiography. Clinical Radiology. 2011;66(7):645-50.
34. Michaud K, Grabherr S, Faouzi M, Grimm J, Doenz F, Mangin P. Pathomorphological and CT-angiographical characteristics of coronary atherosclerotic plaques in cases of sudden cardiac death. International Journal of Legal Medicine. 2015;129(5):1067-77.

35. Ruder TD, Bauer-Kreutz R, Ampanozi G, Rosskopf AB, Pilgrim TM, Weber OM, et al. Assessment of coronary artery disease by post-mortem cardiac MR. Eur J Radiol. 2012;81(9):2208-14.
36. Filograna L, Laberke P, Ampanozi G, Schweitzer W, Thali MJ, Bonomo L. Role of post-mortem computed tomography (PMCT) in the assessment of the challenging diagnosis of pericardial tamponade as cause of death in cases with hemopericardium. Radiol Med. 2015;120(8):723-30.
37. Shiotani S, Watanabe K, Kohno M, Ohashi N, Yamazaki K, Nakayama H. Postmortem computed tomographic (PMCT) findings of pericardial effusion due to acute aortic dissection. Radiation Medicine - Medical Imaging and Radiation Oncology. 2004;22(6):405-7.
38. Watanabe S, Hyodoh H, Shimizu J, Okazaki S, Mizuo K, Rokukawa M. Classification of hemopericardium on postmortem CT. Legal Medicine. 2015;17(5):376-80.
39. Ebert LC, Schön CA, Ruder TD, Thali MJ, Hatch GM. Fatal Left Ventricular Rupture and Pericardial Tamponade Following a Horse Kick to the Chest. The American Journal of Forensic Medicine and Pathology. 2012;33(2).
40. Ruder TD, Ketterer T, Preiss U, Bolliger M, Ross S, Gotsmy WF, et al. Suicidal knife wound to the heart: challenges in reconstructing wound channels with post mortem CT and CT-angiography. Leg Med (Tokyo). 2011;13(2):91-4.
41. Ampanozi G, Flach PM, Ruder TD, Filograna L, Schweitzer W, Thali MJ, et al. Differentiation of hemopericardium due to ruptured myocardial infarction or aortic dissection on unenhanced postmortem computed tomography. Forensic Sci Med Pathol. 2017;13(2):170-6.
42. Ross SG, Thali MJ, Bolliger S, Germerott T, Ruder TD, Flach PM. Sudden Death after Chest Pain: Feasibility of Virtual Autopsy with Postmortem CT Angiography and Biopsy. Radiology. 2012;264(1):250-9.
43. Burke MP, Bedford P, Baber Y. Can Forensic Pathologists Diagnose Pulmonary Thromboembolism on Postmortem Computed Tomography Pulmonary Angiography? The American Journal of Forensic Medicine and Pathology. 2014;35(2).
44. Ampanozi G, Held U, Ruder TD, Ross SG, Schweitzer W, Fornaro J, et al. Pulmonary thromboembolism on unenhanced postmortem computed tomography: Feasibility and findings. Leg Med (Tokyo). 2016;20:68-74.
45. Mueller SL, Thali Y, Ampanozi G, Flach PM, Thali MJ, Hatch GM, et al. Distended diameter of the inferior vena cava is suggestive of pulmonary thromboembolism on unenhanced post-mortem CT. Journal of Forensic Radiology and Imaging. 2015;3(1):38-42.
46. von Both I, Bruni SG, Herath JC. Differentiation of antemortem pulmonary thromboembolism and postmortem clot with unenhanced MRI: a case report. Forensic Sci Med Pathol. 2018;14(1):95-101.

47. Jackowski C, Grabherr S, Schwendener N. Pulmonary thrombembolism as cause of death on unenhanced postmortem 3T MRI. Eur Radiol. 2013;23(5):1266-70.
48. Daily PO, Trueblood HW, Stinson EB, Wuerflein RD, Shumway NE. Management of Acute Aortic Dissections. The Annals of Thoracic Surgery. 1970;10(3):237-47.
49. Ampanozi G, Flach PM, Fornaro J, Ross SG, Schweitzer W, Thali MJ, et al. Systematic analysis of the radiologic findings of aortic dissections on unenhanced postmortem computed tomography. Forensic Sci Med Pathol. 2015;11(2):162-7.
50. Schwendener N, Mund M, Jackowski C. Type II DeBakey dissection with complete aortic rupture visualized by unenhanced postmortem imaging. Forensic Science International. 2013;225(1):67-70.
51. Makino Y, Yamamoto S, Shiotani S, Hayakawa H, Fujimoto H, Yokota H, et al. Can ruptured abdominal aortic aneurysm be accurately diagnosed as the cause of death without postmortem computed tomography when autopsies cannot be performed? Forensic Sci Int. 2015;249:107-11.
52. Yamazaki K, Shiotani S, Ohashi N, Doi M, Kikuchi K, Nagata C, et al. Comparison between computed tomography (CT) and autopsy findings in cases of abdominal injury and disease. Forensic Science International. 2006;162(1):163-6.
53. Arai A, Shiotani S, Yamazaki K, Nagata C, Kikuchi K, Suzuki M, et al. Postmortem computed tomographic (PMCT) and postmortem magnetic resonance imaging (PMMRI) demonstration of fatal massive retroperitoneal hemorrhage caused by abdominal aortic aneurysm (AAA) rupture. Radiation medicine. 2006;24(2):147-9.
54. Paulson EK, Thompson WM. Review of Small-Bowel Obstruction: The Diagnosis and When to Worry. 2015;275(2):332-42.
55. Rami Reddy SR, Cappell MS. A Systematic Review of the Clinical Presentation, Diagnosis, and Treatment of Small Bowel Obstruction. Current Gastroenterology Reports. 2017;19(6):28.
56. Feldman D. The Coffee Bean Sign. 2000;216(1):178-9.
57. Yigit M, Turkdogan KA. Coffee bean sign, whirl sign and bird's beak sign in the diagnosis of sigmoid volvulus. The Pan African medical journal. 2014;19:56.
58. Gascho D, Schaerli S, Tuchtan-Torrents L, Thali MJ, Gorincour G. Use of Postmortem Computed Tomography to Detect Bowel Obstruction and its Relationship to the Cause of Death. Am J Forensic Med Pathol. 2018;39(1):30-7.
59. Baumeister R, Gauthier S, A. Bolliger S, J. Thali M, G. Ross S. Forensic imaging in an unusual postmortem case of sigmoid volvulus. Journal of Forensic Radiology and Imaging. 2015;3(3):186-8.

60. Usui A, Kawasumi Y, Hosokai Y, Ishizuka Y, Ikeda T, Saito H, et al. A case of fatal sigmoid volvulus visualized on postmortem radiography: The importance of image optimization with multidetector computed tomography. Legal Medicine. 2016;19:32-4.
61. Dagradi AE. Gastrointestinal Hemorrhage. Journal of Clinical Gastroenterology. 1981;3(3).
62. Gershon A, Little DA, Ball CG, Williams AS. Fatal secondary aortoduodenal fistula diagnosed with postmortem computed tomography angiography. Forensic Science, Medicine and Pathology. 2020;16(3):515-8.
63. Fliss B, Bartsch C, Flach PM, Thali MJ, Ampanozi G. Fatal aorto-esophageal fistula detected on postmortem computed tomography angiography. Journal of Forensic Radiology and Imaging. 2015;3(3):182-5.
64. Williams AS, Little DAL, Herath J. Sudden unexpected death as a result of primary aortoduodenal fistula identified with postmortem computed tomography. Forensic Science, Medicine, and Pathology. 2015;11(4):596-600.
65. Suzuki H, Hasegawa I, Hoshino N, Fukunaga T. Two forensic autopsy cases of death due to upper gastrointestinal hemorrhage: A comparison of postmortem computed tomography and autopsy findings. Legal Medicine. 2015;17(3):198-200.
66. Ampanozi G, Schumann K, Thali MJ, Gascho D. Aortojejunal fistula. Journal of Forensic Radiology and Imaging. 2015;3(1):101.
67. bin Abdul Rashid SN, Bouwer H, O'Donnell C. Lethal hemorrhage from a ureteric–arterial–enteric fistula diagnosed by postmortem CT angiography. Forensic Science, Medicine, and Pathology. 2012;8(4):430-5.
68. Ziai WC, Carhuapoma JR. Intracerebral Hemorrhage. CONTINUUM: Lifelong Learning in Neurology. 2018;24(6):1603-22.
69. Morales H. Pitfalls in the Imaging Interpretation of Intracranial Hemorrhage. Semin Ultrasound CT MR. 2018;39(5):457-68.
70. Smith SD, Eskey CJ. Hemorrhagic stroke. Radiol Clin North Am. 2011;49(1):27-45.
71. Tappero C, Thali MJ, Schweitzer W. The possibility of identifying brain hemorrhage in putrefied bodies with PMCT. Forensic Science, Medicine and Pathology. 2020:1 - 6.
72. Ferrante E, Regna-Gladin C, Arpino I, Rubino F, Porrinis L, Ferrante MM, et al. Pseudo-subarachnoid hemorrhage: A potential imaging pitfall associated with spontaneous intracranial hypotension. Clinical Neurology and Neurosurgery. 2013;115(11):2324-8.
73. Shirota G, Gonoi W, Ikemura M, Ishida M, Shintani Y, Abe H, et al. The pseudo-SAH sign: an imaging pitfall in postmortem computed tomography. Int J Legal Med. 2017;131(6):1647-53.

74. Aguilar MI, Brott TG. Update in intracerebral hemorrhage. Neurohospitalist. 2011;1(3):148-59.
75. Nolte KB, Brass LM, Fletterick CF. Intracranial hemorrhage associated with cocaine abuse. Neurology. 1996;46(5):1291.
76. Yen K, Lövblad KO, Scheurer E, Ozdoba C, Thali MJ, Aghayev E, et al. Post-mortem forensic neuroimaging: correlation of MSCT and MRI findings with autopsy results. Forensic Sci Int. 2007;173(1):21-35.
77. Berger N, Ebert LC, Ampanozi G, Flach PM, Gascho D, Thali MJ, et al. Smaller but denser: postmortem changes alter the CT characteristics of subdural hematomas. Forensic Sci Med Pathol. 2015;11(1):40-6.
78. Añon J, Remonda L, Spreng A, Scheurer E, Schroth G, Boesch C, et al. Traumatic extra-axial hemorrhage: correlation of postmortem MSCT, MRI, and forensic-pathological findings. J Magn Reson Imaging. 2008;28(4):823-36.
79. Kobayashi T, Shiotani S, Kaga K, Saito H, Saotome K, Miyamoto K, et al. Characteristic signal intensity changes on postmortem magnetic resonance imaging of the brain. Japanese Journal of Radiology. 2010;28(1):8-14.
80. Giovane RA, Lavender PD. Central Nervous System Infections. Prim Care. 2018;45(3):505-18.
81. Liu K, Yang C, Zhang Y, Yuan X, Xiao H, Bai Ya, et al. Brain Abscess Following Intracerebral Hemorrhage in a Patient With Pneumonia. Journal of Craniofacial Surgery. 2016;27(8):e773-e5.
82. Thurnher MM, Sundgren PC. IDKD Springer Series Intracranial Infection and Inflammation. In: Hodler J, Kubik-Huch RA, von Schulthess GK, editors. Diseases of the Brain, Head and Neck, Spine 2020–2023: Diagnostic Imaging. Cham (CH): Springer Copyright 2020, The Author(s). 2020. p. 59-76.
83. Thurnher MM. Infections in Immunocompromised Individuals. In: Barkhof F, Jager R, Thurnher M, Rovira Cañellas A, editors. Clinical Neuroradiology: The ESNR Textbook. Cham: Springer International Publishing; 2018. p. 1-32.
84. Noriki S, Kinoshita K, Inai K, Sakai T, Kimura H, Yamauchi T, et al. Newly recognized cerebral infarctions on postmortem imaging: a report of three cases with systemic infectious disease. BMC Med Imaging. 2017;17(1):4-.
85. Chatzaraki V, Bolliger SA, Thali MJ, Eggert S, Ruder TD. Unexpected brain finding in pre-autopsy postmortem CT. Forensic Science, Medicine and Pathology. 2017;13(3):367-71.
86. Heimer J, Gascho D, Chatzaraki V, Knaute DF, Sterzik V, Martinez RM, et al. Postmortem (1)H-MRS-Detection of Ketone Bodies and Glucose in Diabetic Ketoacidosis. Int J Legal Med. 2018;132(2):593-8.
87. Heimer J, Gascho D, Madea B, Steuer A, Martinez R, Thali M, et al. Comparison of the beta-hydroxybutyrate, glucose, and lactate concentrations derived from postmortem proton magnetic resonance spectroscopy and

biochemical analysis for the diagnosis of fatal metabolic disorders. International Journal of Legal Medicine. 2020;134.
88. Ben Salem D, Perouse De Montclos E, Couaillier JF, Martin D, Krause D, Brunotte F, et al. [Neuroradiologic emergencies in infectious pathology]. J Neuroradiol. 2004;31(4):301-12.
89. Mountford CE, Stanwell P, Lin A, Ramadan S, Ross B. Neurospectroscopy: the past, present and future. Chem Rev. 2010;110(5):3060-86.
90. Shiotani S, Kohno M, Ohashi N, Yamazaki K, Nakayama H, Watanabe K, et al. Non-traumatic postmortem computed tomographic (PMCT) findings of the lung. Forensic Sci Int. 2004;139(1):39-48.
91. Robinson C, Biggs MJ, Amoroso J, Pakkal M, Morgan B, Rutty GN. Post-mortem computed tomography ventilation; simulating breath holding. International Journal of Legal Medicine. 2014;128(1):139-46.
92. Germerott T, Preiss US, Ebert LC, Ruder TD, Ross S, Flach PM, et al. A new approach in virtopsy: Postmortem ventilation in multislice computed tomography. Leg Med (Tokyo). 2010;12(6):276-9.
93. Filograna L, Thali MJ. Post-mortem CT imaging of the lungs: pathological versus non-pathological findings. Radiol Med. 2017;122(12):902-8.
94. Ampanozi G, Schwendener N, Krauskopf A, Thali MJ, Bartsch C. Incidental occult gunshot wound detected by postmortem computed tomography. Forensic Sci Med Pathol. 2013;9(1):68-72.
95. Weustink AC, Hunink MG, van Dijke CF, Renken NS, Krestin GP, Oosterhuis JW. Minimally invasive autopsy: an alternative to conventional autopsy? Radiology. 2009;250(3):897-904.
96. Gupta D, Hansell A, Nichols T, Duong T, Ayres JG, Strachan D. Epidemiology of pneumothorax in England. Thorax. 2000;55(8):666-71.
97. Global Health Estimates 2016: Deaths by Cause, Age, Sex, by Country and by Region, 2000-2016. Geneva: World Health Organization; 2018 [Available from: https://www.who.int/news-room/fact-sheets/detail/the-top-10-causes-of-death.
98. Lanks CW, Musani AI, Hsia DW. Community-acquired Pneumonia and Hospital-acquired Pneumonia. Medical Clinics of North America. 2019;103(3):487-501.
99. Suárez I, Fünger SM, Kröger S, Rademacher J, Fätkenheuer G, Rybniker J. The Diagnosis and Treatment of Tuberculosis. Dtsch Arztebl International. 2019;116(43):729-35.
100. Ishiguro T, Yoshii Y, Kanauchi T, Hoshi T, Takaku Y, Kagiyama N, et al. Re-evaluation of the etiology and clinical and radiological features of community-acquired lobar pneumonia in adults. J Infect Chemother. 2018;24(6):463-9.

101. Pascarella G, Strumia A, Piliego C, Bruno F, Del Buono R, Costa F, et al. COVID-19 diagnosis and management: a comprehensive review. J Intern Med. 2020;288(2):192-206.
102. Traill Z. The role of computed tomography and magnetic resonance imaging in the investigation of natural death. Diagnostic Histopathology. 2010;16(12):560-4.
103. Gonoi W, Watanabe Y, Shirota G, Abe H, Okuma H, Shintani-Domoto Y, et al. Pulmonary postmortem computed tomography of bacterial pneumonia and pulmonary edema in patients following non-traumatic in-hospital death. Legal Medicine. 2020;45:101716.
104. McLaughlin S, Kind K, Thomson L, Bouhaidar R. Unexpected active tuberculosis on Post Mortem CT: A case report and review of the literature. Forensic Science International. 2016;266:e64-e7.
105. Heron M, Anderson RN. Changes in the Leading Cause of Death: Recent Patterns in Heart Disease and Cancer Mortality. NCHS Data Brief. 2016(254):1-8.
106. Heron M. Deaths: Leading Causes for 2015. Natl Vital Stat Rep. 2017;66(5):1-76.
107. Piccioli A, Maccauro G, Spinelli MS, Biagini R, Rossi B. Bone metastases of unknown origin: epidemiology and principles of management. J Orthop Traumatol. 2015;16(2):81-6.
108. Hutchinson BD, Shroff GS, Truong MT, Ko JP. Spectrum of Lung Adenocarcinoma. Seminars in Ultrasound, CT and MRI. 2019;40(3):255-64.
109. Makary MA, Daniel M. Medical error—the third leading cause of death in the US. BMJ. 2016;353:i2139.
110. Parajuli S, Aneja A, Mukherjee A. Undiagnosed fatal malignancy in adult autopsies: a 10-year retrospective study. Hum Pathol. 2016;48:32-6.
111. Vester MEM, van Rijn RR, Duijst W, Beenen LFM, Clerkx M, Oostra RJ. Added value of post-mortem computed tomography (PMCT) to clinical findings for cause of death determination in adult "natural deaths". Int J Legal Med. 2019.
112. O'Brien J, Jones N, Horrigan M, Al-Kaisey AM. Rare cause of pulmonary hypertension - pulmonary tumour thrombotic microangiopathy. BMJ Case Rep. 2019;12(8).
113. Takahashi N, Higuchi T, Shiotani M, Maeda H, Sasaki O. Multiple lung tumors as the cause of death in a patient with subarachnoid hemorrhage: postmortem computed tomography study. Jpn J Radiol. 2009;27(8):316-9.
114. Diabetes [updated 08.06.2020. Available from: https://www.who.int/news-room/fact-sheets/detail/diabetes

115. Püschel K. Plötzlicher Tod im Erwachsenenalter. In: B. Brinkmann MM, editor. Handbuch Der Gerichtlichen Medizin 1. Berlin: Springer; 2004. p. 965–1070.
116. Ruder TD, Schweitzer W, Ampanozi G, Gascho D, Flach PM, Thali MJ, et al. Imaging findings of diabetes on post-mortem CT. Journal of Forensic Radiology and Imaging. 2018;13:27-41.
117. Stasinou T, Bourdoumis A, Owegie P, Kachrilas S, Buchholz N, Masood J. Calcification of the vas deferens and seminal vesicles: a review. Can J Urol. 2015;22(1):7594-8.
118. R. Weissleder JW, M.G. Harisinghani, J.W. Chen. Genitourinary Imaging. In: R Weissleder JW, MG Harisinghani, JW Chen editor. Primer of Diagnostic Imaging. Philadelphia: Mosby Elsevier; 2007. p. 275–364
119. Culver GJ, Tannenhaus J. Calcification of the vas deferens in diabetes. J Am Med Assoc. 1960;173:648-51.

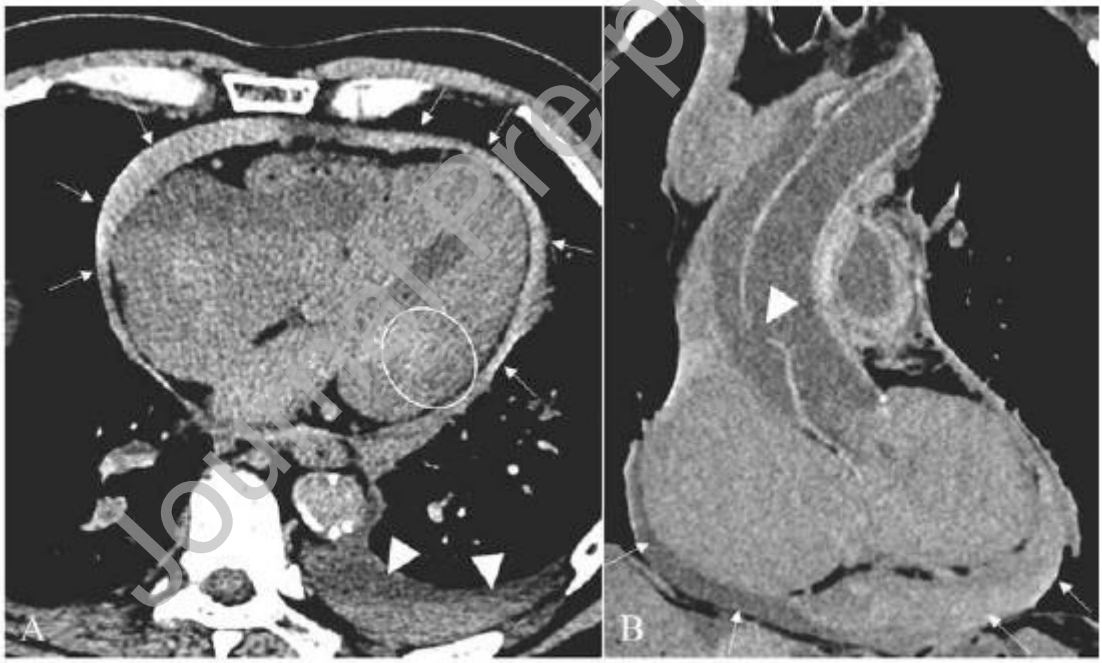

Figure 1

a) Unenhanced PMCT of the heart, axial plane (soft tissue window). Note the presence of hemopericardium (white arrows) and left hemothorax (white arrowheads). An inhomogeneous area of the left free myocardial wall (encircled) suggests myocardial rupture as the cause of the hemopericardium.

b) Unenhanced PMCT of the heart, coronal plane (soft tissue window). Hemopericardium (white arrows) caused by type A dissection of the ascending aorta. Tear of the aortic intimal layer (white arrowhead).

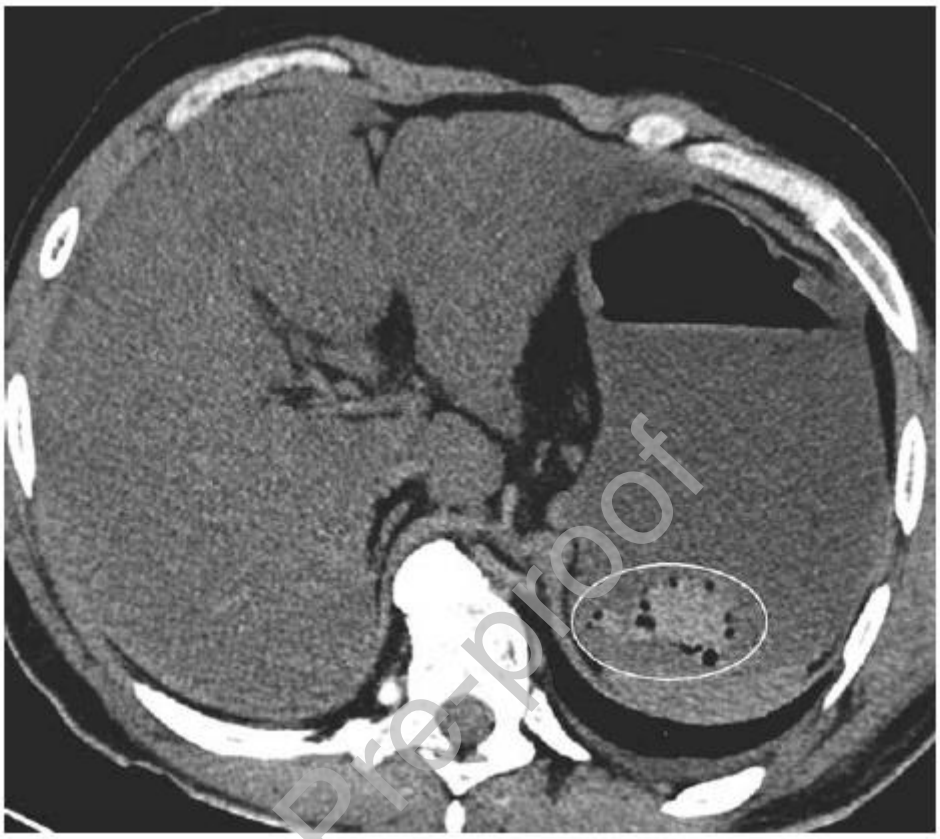

Figure 2

PMCT of the upper abdomen, axial plane (soft tissue window). Stomach content with hyperdense sedimented structure (encircled), suggestive for blood clots. Differentiation of blood clots from other hyperdense stomach contents (eg food) is challenging.

Fig. 3

Unenhanced PMCT of the head, axial plane (soft tissue window). Traumatic subarachnoid hemorrhage (SAH) (black arrows) with blood in the basal cisterns (white arrows) and intraventricular (asterisks). There is little edema.

Fig. 4

Unenhanced PMCT of the head, axial plane (soft tissue window). Pseudo-SAH (arrows) with brain swelling and venous congestion. No intraventricular blood was seen.

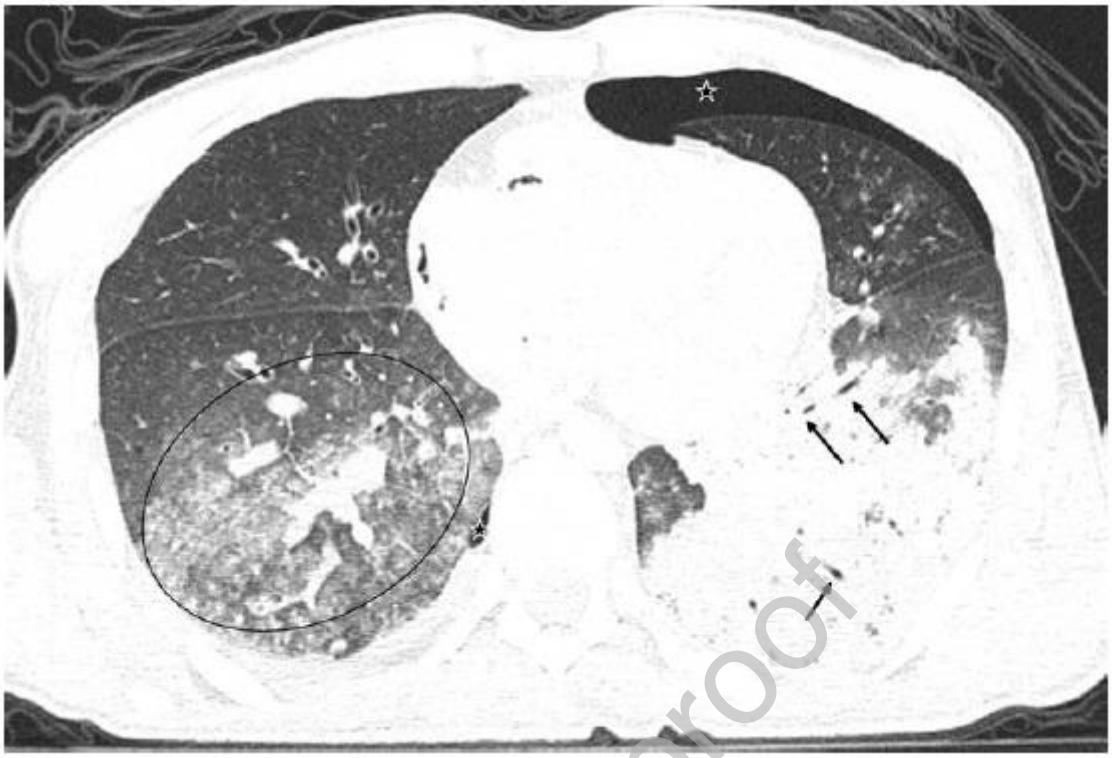

Fig. 5

PMCT of the lung, axial plane (lung window) after aspiration. Consolidation in the left posterobasal lower lobe caused by aspiration pneumonia with air-bronchogram (arrows). Additionally, ground-glass opacities and tree-in bud phenomenon in the right lower lobe posterobasal (ellipse) and little pleural effusion. Note pneumothorax on both sides (asterisks).

Fig. 6

Unenhanced PMCT of the spine (1a) and osseous pelvis (1b), sagittal and axial plane (bone window). 81-year-old deceased with long-time therapy of prostate cancer and diffuse bone metastasis consecutively with osteolytic, hypodense (asterisks) and osteosclerotic, hyperdense (arrows) component. Margins are well-outlined and irregular in both types. Note the more posterior localization of bone metastasis in the vertebral body T3-5. Additional atherosclerotic of the aorta is visible.

Fig. 7

PMCT of the pelvis, axial plane (soft tissue window). Symmetrical vas deferens calcification (arrows) indicating diabetes mellitus.